A Comprehensive Sensitivity Analysis Framework for Model Evaluation and Improvement Using a Case Study of the Rangeland Hydrology and Erosion Model

H. Wei, M. A. Nearing, J. J. Stone

Abstract. *The complexity of numerical models and the large numbers of input factors result in complex interdependencies of sensitivities to input parameter values, and high risk of having problematic or nonsensical model responses in localized regions of the input parameter space. Sensitivity analysis (SA) is a useful tool for ascertaining model responses to input variables. One popular method is local SA, which calculates the localized model response of output to an input parameter. This article describes a comprehensive SA method to explore the parameter behavior globally by calculating localized sensitivity indices over the entire parameter space. This article further describes how to use this framework to identify model deficiencies and improve model function. The method was applied to the Rangeland Hydrology and Erosion Model (RHEM) using soil erosion response as a case study. The results quantified the localized sensitivity, which varied and was interdependently related to the input parameter values. This article also shows that the localized sensitivity indices, combined with techniques such as correlation analysis and scatter plots, can be used effectively to compare the sensitivity of different inputs, locate sensitive regions in the parameter space, decompose the dependency of the model response on the input parameters, and identify nonlinear and incorrect relationships in the model. The method can be used as an element of the iterative modeling process whereby the model response can be surveyed and problems identified and corrected in order to construct a robust model.*

Keywords. *Hydrology, Local sensitivity, Morris' screen method, RHEM, Soil erosion.*

Many numerical models involve the utilization of a large number of input parameters, which often results in complex interactions between inputs and algorithms within the model. In all models, it is generally desirable to understand the relationships between output sensitivities and input parameter values, and how these relationships affect model predictions. This is important not only for gaining a better understanding of the model behavior, but also for detecting model deficiencies and unreasonable responses induced by the high level of model complexity and the high number of model input parameters.

Sensitivity analysis (SA) is a method widely used to ascertain the response of a simulation model to changes in its input parameters. In practice, SA is not only applied to examine the importance of input parameters but is also considered an important element of the model development process. SA helps to elucidate the impact of different model structures, prepare for model parameterization, and direct research priorities by focusing on the parameters that contribute the most to uncertainty to the model response (Saltelli and Campolongo, 2000; Breshears et al., 1992).

Many different SA techniques are available (see reviews and comparisons by Helton, 1993; Campolongo and Saltelli, 1997; Saltelli and Campolongo, 2000; and Ionescu-Bujor and Cacuci, 2004). Methods such as response surface, regional SA, scatter plots, differential analysis, and Monte Carlo analysis may give impressive results, but they are not widely applied due to the lack of quantitative sensitivity indices, or their difficulty in application to complex models (e.g., differential analysis). The most well known SA methodology categories are the so-called local SA and global SA. Local SA, also termed the "one factor at a time" (OAT) or deterministic approach, is a derivative-based method. It aims to quantify the exact local response of output (Y) to a particular input factor (x_i) at a selected point (x^0) within the full input parameter space for the model. The most common form of a local sensitivity index is:

$$\left\{\frac{\partial Y}{\partial x_i}\right\}_{x^0} = \frac{Y(x_1^0, \ldots, x_i^0 + \partial x_i, \ldots, x_I^0) - Y(x^0)}{\partial x_i} \qquad (1)$$

where $i = (1, \ldots, I)$, and I is the number of total input parameters. The local sensitivity index measures the partial derivatives of Y with respect to x_i at point x^0. Alternative forms of the technique measure the effect on Y of perturbing the x_i values by either a fixed amount (e.g., a fixed percent) or by some estimate of the standard deviation of the input (Saltelli and Campolongo, 2000).

The concept of local sensitivity analysis is simple, and it is effective if the localized sensitivity is of interest. However,

Submitted for review in December 2006 as manuscript number SW 6797; approved for publication by the Soil & Water Division of ASABE in March 2007.

The authors are **Haiyan Wei,** Research Specialist, **Mark A. Nearing,** Research Leader, and **Jeffry J. Stone,** Research Hydrologist, USDA-ARS Southwest Watershed Research Center, Tucson, Arizona. **Corresponding author:** Haiyan Wei, USDA-ARS Southwest Watershed Research Center, 2000 E Allen Rd., Tucson, AZ 85719; phone: 520-670-6381, ext. 145; e-mail: hwei@tucson.ars.ag.gov.

if the modeler wants information on the overall effect of an input factor on the model, the limitation of this derivative-based method is evident: it is not a representative overall sensitivity index for most numerical models that involve nonlinear relationships and strong interactions (Saltelli and Campolongo, 2000). For a non-linear model, the local sensitivity index is invalid if the chosen ∂x_i is too large. This has been demonstrated by Breshears et al. (1992). When he conducted a sensitivity analysis based on different ranges of ∂x_i, the sensitivity index varied; thus, the local sensitivity index was demonstrated to be a magnitude-based index. For a model with strong interactions due to the dependency of one parameter on the others, the modeler must obtain various local sensitivity indices for a specific factor x_i at different points x^0.

Global SA was so named because it considers and calculates the total effect of a parameter on a model across the entire parameter space. Most of the global SA methods are variance-based, i.e., the global sensitivity index is represented by the contribution of each input factor to the total variance of the model output. The Fourier amplitude sensitivity test (FAST, and the extended FAST) is one of the variance-based global SA approaches, and it has been successfully applied in many different fields (Helton, 1993; Saltelli and Campolongo, 2000; Crosetto and Tarantola, 2001). An alternative global SA approach, called multi-objective generalized sensitivity analysis (MOGSA), is based on an extension of regional sensitivity analysis (Hornberger and Spear, 1981). MOGSA investigates the sensitivities of individual parameters by examining whether a prior distribution of the parameters separates under a specific behavioral classification via a K-S probability index (Liu et al., 2004).

In contrast to global SA, local SA does not help to capture the overall effect of an input factor on a model output, but it is the only way to investigate the parameter sensitivity for specific input scenarios. This is especially important for complex models that involve non-linear effects or strong interactive relationships. For such complex models, the effect of a given parameter may be highly localized; hence, an overall sensitivity index will not be applicable to every case and will be misleading in many cases (i.e., regions of the input parameter space).

The localized sensitivity concept has been employed to build very useful tools, such as Morris' screening method (Morris, 1991), the forward sensitivity analysis procedure (FSAP) of Ionescu-Bujor and Cacuci (2004), and the adjoint sensitivity analysis procedure (ASAP). The method of Morris is widely used to identify key parameters (Saltelli and Campolongo, 2000; Francos et al., 2003). It divides the range of each input parameter x_i into p levels, using Latin hypercube randomly sampled points from the $p \times I$ parameter space (I is the number of the parameters) and calculates the "elementary effect" using equation 1, with ∂x_i the predetermined multiple of $1/(p-1)$. For each x_i, the elementary effects associated with each selected point will form a distribution. The advantage of this method is that the estimates of the means and standard deviations of the distributions can be used as indicators of the importance of the input parameters. A large mean indicates an important overall influence on the output. A large standard deviation indicates that the influence is highly dependent on the values of the inputs, and that the effect is either non-linear or highly dependent on other factors.

Morris provided an effective framework for analyzing local sensitivity across the entire parameter space. However, the elementary effect of Morris uses a multiple of $1/(p-1)$ as the change in the input factor (∂x_i), which does not always ensure that the elementary effect is representative of the exactly localized response of the output at point x^0. This also limits application of this method beyond the screening of the input factors.

The objective of this article is to provide a new local sensitivity analysis framework that can be used effectively to show the interdependencies of sensitivity to multiple model inputs, and which can be used in the model development process to help identify undesirable or illogical model responses. This study uses an algorithm similar to Morris' framework, but uses a different local sensitivity index to build a localized sensitivity matrix over the entire parameter space. The sensitivity matrix is further analyzed to make SA more effective as an aid in the model development process. In this article, we illustrate the use of this framework to: (1) examine the localized sensitivity to each parameter, and list and classify the importance of the input parameters; (2) locate the sensitive region for an input parameter; (3) decompose the dependency of model response on input parameter values to understand the parameter interactions, using correlations and regressions; and (4) generate scatter plots to survey the model response and reveal the nonlinear relationships, thresholds, and potential weaknesses or problems of the model structure.

This article, taking the erosion predictions in the Rangeland Hydrology and Erosion Model (RHEM) as an example, not only highlights the local sensitivities, but also describes how to investigate the interactions between RHEM parameters and how to identify unusual RHEM behavior. Results from this study will be helpful in improving the understanding of the model behavior and parameter interactions in RHEM, and in improving the integrity of the model predictions.

METHODOLOGY

SENSITIVITY EQUATION

The local sensitivity index in this article is quantified by the following equation:

$$S_{i_{(x^0)}} = \frac{\dfrac{Y(x_1^0,\ldots,x_i^0+\partial x_i,\ldots,x_I^0)-Y(x^0)}{Y(x^0)}}{\dfrac{\partial x_i}{x_i^0}} \qquad (2)$$

where $S_{i_{(x^0)}}$ is the sensitivity of output Y to input factor x_i at point $x^0(x_1^0,\ldots,x_i^0,\ldots,x_I^0)$; $S_{i_{(x^0)}}$ is a non-dimensional, localized index that represents the normalized response of the output to an increase in input value x_i. The absolute magnitude of $S_{i_{(x^0)}}$ indicates the degree of sensitivity of Y to x_i at point x^0. A positive (or negative) S_i indicates a positive (or negative) relationship between Y and x_i, i.e., an increase in x_i will cause an increase in Y. The percentage of $\partial x_i / x_i^0$ is expected to be small enough to ensure that S_i is representative at point x^0. One of the merits of equation 2 is that if $\partial x_i / x_i^0$ remains a constant percentage, then the value of $S_{i_{(x^0)}}$ can be

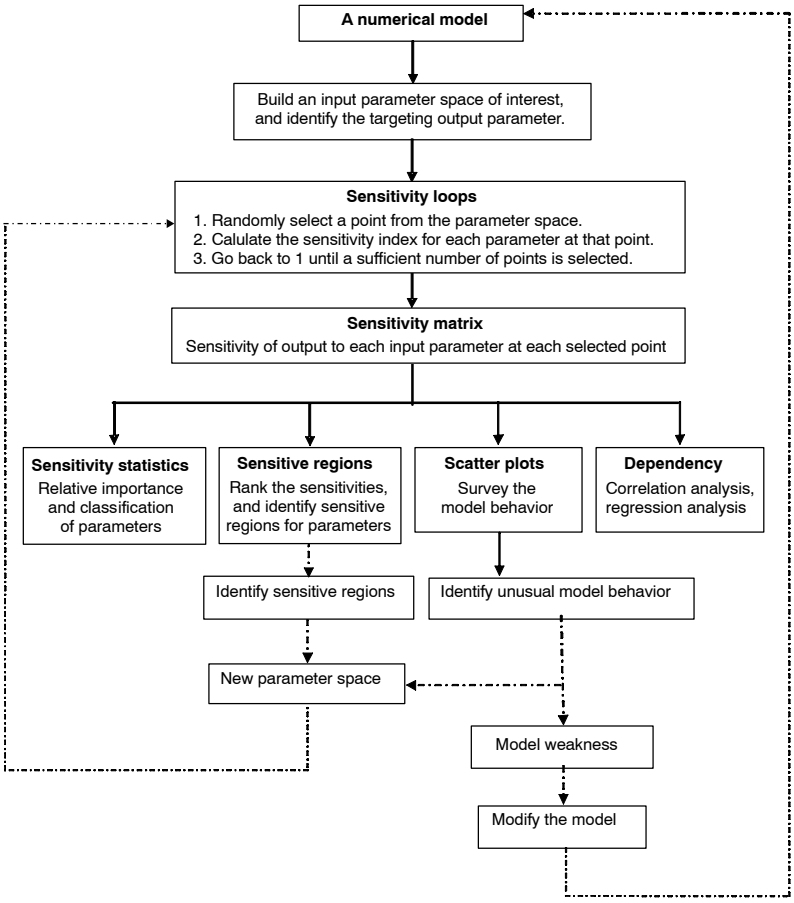

Figure 1. Flowchart of the sensitivity analysis described in this article.

used to compare the sensitivity of the output to an input variable at its different magnitudes. It can also be used to compare the sensitivity of the output to different individual input factors, for example, the sensitivity of Y to x_i and x_j at point x^0.

Procedure

Figure 1 is a flowchart of the methodology used in this article. It starts with selecting the input and output parameters to be analyzed. The ranges of each input parameter should then be given to build the parameter space of interest, which can encompass the full realistic range of all input parameters. Points x^0 were then randomly selected from the parameter space, and sensitivity indices were calculated for each parameter at the selected point. Latin hypercube (LH) sampling (McKay et al., 1979) was used for random sampling of points x^0. At each point selected by LH, the model was run $(1 + I)$ times. The first run was used to calculate and save the output value at point x^0 with no perturbation, and the next I runs were used to calculate new output values after increasing each parameter, one at a time, by a predetermined percentage $(\partial x_i / x_i^0)$. The local sensitivity index for each input parameter at this point was then calculated using equation 2 based on the $(1 + I)$ values of the output at this point.

In this study, the sampling procedure and local sensitivity index calculation were repeated 10,000 times, after which the parameter space was well covered and the points were well distributed. At the conclusion of the runs, a sensitivity index matrix had been constructed from the results, containing the values of each parameter at each selected point and the local sensitivity of the output to each input parameter at each point. The absolute values of the sensitivities were also generated for further analysis. A Fortran program was written to connect the model, the LH sampling, the sensitivity loops, and the building of the sensitivity matrix.

The sensitivity matrix was used for further analysis. It was first used to examine the localized sensitivity for each parameter over the whole parameter space. The estimated means and standard deviations of the distributions of each S_i were used to rank and classify the effects of the parameters. The sensitivity matrix was also used to identify if there were contiguous sensitive regions for particular parameters. The sensitivity index (S_i) and the model output were plotted to examine the model response at different output values. Sensitivities for different input parameters (S_i and S_j) were plotted to analyze the relationship between two parameters. Regression and correlation analysis were conducted to analyze the dependency of sensitivity (S_i) on the input parameter values. Scatter plots of S_i versus the value of the ith input parameter were generated to identify unusual model responses and model weaknesses.

Latin Hypercube Sampling

Latin hypercube (LH) sampling (McKay et al., 1979; Stein, 1987) was used to select random points from the uniformly distributed parameter space. McKay et al. (1979) compared several sampling techniques, and they concluded that the LH method had a number of desirable advantages over the other techniques. LH first divides the range of each

input variable into N strata of equal probability $1/N$, and then samples a value from each stratum randomly. The values of each input variable are combined at random to locate a point in the parameter space. One of the advantages of this method that makes it appropriate for this study is that LH ensures full coverage over the range of each variable so that all areas of the sample space will be represented by the selected input values.

RHEM Model and Input Parameter Space

The Rangeland Hydrology and Erosion Model (RHEM) was developed from the Water Erosion Prediction Project (WEPP) model (Flanagan and Nearing, 1995; Nearing et al., 1989; Laflen et al., 1997). It predicts the hydrology, erosion, and deposition from single storms based on fundamentals of infiltration, surface runoff, hydraulics, and erosion mechanics on the hillslope scale. In this study, we selected 14 input parameters used in the hydrology and erosion components of RHEM for the sensitivity analysis. The amount of soil erosion from the hillslope, *soil loss* (kg/m^2), was selected as the targeted output variable. The parameter space of interest for this study is the entire applicable space of the RHEM model. Thus, the full range of all reasonable values that might occur for each input parameter was used to build a 14-dimensional parameter space (table 1). The ranges were based on recommendations in the WEPP manual (Flanagan and Livingston, 1995) and the WEPP database (Elliot et al., 1989; Simanton et al., 1991; Laflen et al., 1991; Alberts et al., 1995).

Table 1 lists the name, range, and description of each input parameter studied. The range of each input parameter was required for the sensitivity study. The slope gradient (*slp*) and slope length (*sln*) were the two parameters that represent the slope condition. The rainfall parameters included storm total rainfall (*rain*), peak rainfall intensity divided by average intensity (*xip*), and storm duration (*dur*). Hydraulic parameters were the Green-Ampt Mein-Larsen hydraulic conductivity (*ke*) and effective matric potential (*ns*). Erosion parameters were the interrill erodibility coefficient (*ki*), the rill erodibility coefficient (*kr*), and critical shear stress (τ_c). Friction parameters were runoff friction (*fr*) and erosion friction (*fe*). Rill spacing on the hillslope was *rsp*. The particle size distribution parameter (*psd*) was used in the model to build a lognormal distribution curve, from which five pairs of particle size and fraction data were obtained and passed to the transport capacity and deposition calculations. Building a lognormal distribution curve requires the values of the mean and standard deviation; *psd* is the mean value, and it is always negative due to the logarithm transformation. A constant standard deviation of 2.163 was used for the distribution of all types of sediments, which was based on the WEPP database (Elliot et al., 1989; Simanton et al., 1991; Laflen et al., 1991; Alberts et al., 1995).

Table 1. Parameters and parameter ranges used in this study.

Input Parameter	Lower Bound	Upper Bound	Unit	Description
slp	3	30	%	Slope
sln	10	100	m	Slope length
rain	20	120	mm	Rainfall volume
dur	0.5	2	h	Rainfall duration
xip	1	20	--	Rainfall peak intensity variable
ki	1000	2×10^6	kg*s/m^4	Interrill erodibility
kr	0.00001	0.004	s/m	Rill erodibility
τ_c	0.0001	7	N/m^2	Critical shear stress
ke	0.8	40	mm/h	Effective hydraulic conductivity
ns	0.00025	0.7	m	Matric potential
fr	4.07	200	--	Friction factor for runoff
fe	1.11	100	--	Friction factor for erosion
rsp	0.5	5	m	Rill spacing
psd	−7	−1	--	Particle size distribution

The increment of each input parameter and the total number of samples were also required for the SA program. The increment was arbitrarily set at 5% in this study. A small value of the increment is preferred to make the sensitivity index representative of the exact localized effect, but the increment must be large enough to avoid rounding errors in the calculations. The total number of points should be determined by considering not only the number of the input parameters but the complexity of the model. In this study, 10,000 points were used as a representative sampling of the full input parameter space.

Results

Approximately 50% of the 10,000 events did not generate rainfall excess, which means that runoff and erosion from these events was zero, and approximately 20% of the events yielded runoff less than 5 mm, which was considered to be too small to be of interest in terms of output. As a result, only the 3180 events (of the 10,000 total events) that generated runoff greater than 5 mm were saved in the sensitivity matrix for further analysis. The rainfall excess regime is mathematically complicated and is controlled in the model by the relationships between the rainfall and infiltration processes, which is why only a portion of the combinations of the input parameters yielded runoff events of interest. This result is important because it is probably true for many numerical models that only a portion of the entire parameter space yields relevant results, and it is always interesting to know what this proportion is and where it is located in the entire parameter space.

To reveal the location of the parameter space of interest, we compared the histograms of each parameter in the entire parameter space with that in the saved sensitivity matrix. The distributions of all parameters in the entire parameter space fell into uniform distributions according to the LH sampling method used in this study. However, the results showed that the distribution of some parameters changed after screening out the non-significant events. For example, figure 2 shows two distributions of the input parameter *rain*. Figure 2a shows the distribution of *rain* in the parameter space of 10,000 events, and figure 2b shows the distribution of *rain* in the parameter space of the 3180 events that produced runoff greater than 5 mm. It can be seen that many events with small *rain* values were removed. In addition to *rain*, we found that some events with high *ke* and *ns* values were also removed. This indicates that these three parameters control the amount of runoff.

Localized Sensitivity

Absolute local sensitivity can be used to compare the relative importance of the input parameters. Each row of the sensitivity matrix generates a ranking of parameter importance based on the rank of the absolute sensitivity values at each point. However, the importance of a parameter varied from point to point. For example, at point 23, the ranking of the pa–

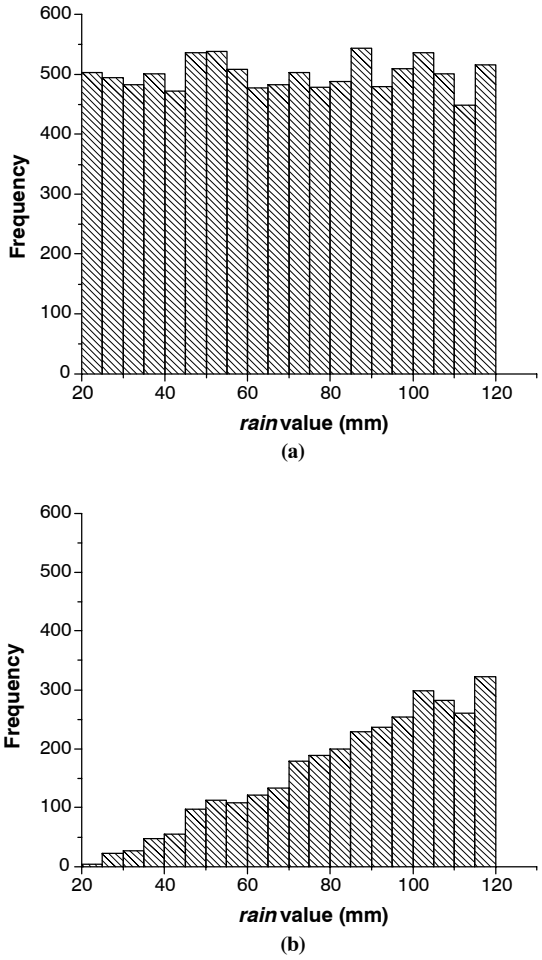

Figure 2. Distributions of parameter *rain* (a) in the whole parameter space and (b) in the parameter space of interest.

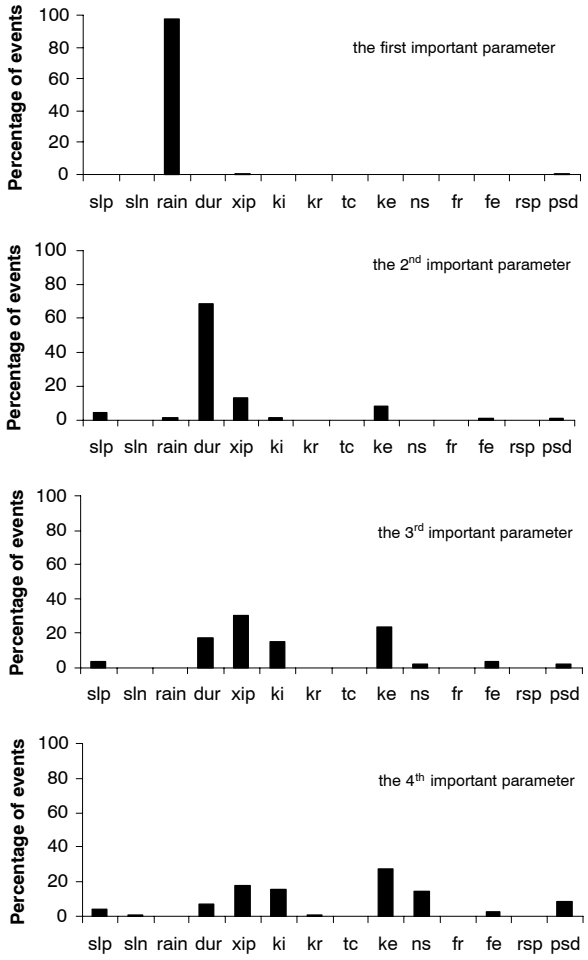

Figure 3. Distribution of the four top-ranked input parameters based on the count of events. The top graph shows that *rain* was the most sensitive parameter for 97.99% of the events, with *psd*, *dur*, *xip*, *slp*, τ_c, and *ke* the most sensitive parameters for the remaining 2.01% of the events.

rameters was: *rain*, *dur*, *ke*, *ns*, *xip*, *ki*, *sln*, *psd*, *slp*, *fe*, *fr*, *rsp*, *kr*, and τ_c. At point 30, the ranking was: *psd*, *rain*, *dur*, *xip*, *ke*, *ki*, *ns*, *slp*, *fe*, *sln*, *fr*, *rsp*, *kr*, and τ_c. Figure 3 lists the four most important parameters based on the count of events. For 98.0% of the 3180 events, the total rainfall depth (*rain*) was the most important parameter, but *psd*, *dur*, *xip*, *slp*, τ_c, and *ke* also showed up as top-ranked parameters, and these parameters accounted for the remaining 2.0% of the events. Storm duration (*dur*) was the second most sensitive parameter for 68.5% of the total events, and *slp*, *rain*, *xip*, *ki*, *kr*, *ke*, *fe*, and *psd* accounted for the rest (31.5%) of the events. The third and fourth ranked parameters were more widely distributed among the input parameters (fig. 3). The results show that for a complex model in which the input parameters interact with each other, the sensitivity for input parameters may vary greatly from point to point in the parameter space.

Classification of Input Parameter Effects

The distribution of the sensitivities (S_i) for each input parameter can be generated from the sensitivity matrix, and the characteristics of the distributions can be used to address and classify the effects of the input parameters on the model output (Morris, 1991; Saltelli and Campolongo, 2000). The mean of S_i describes the overall effect of the parameter on model response, and the standard deviation of S_i, which indicates the spread tendency of S_i, describes the interaction or nonlinear effect of the parameter.

Figure 4 shows the distribution of each S_i based on absolute values. The parameters are listed by the ranking of their mean sensitivities for the overall effect: *rain*, *dur*, *xip*, *ke*, *ns*, *ki*, *psd*, *slp*, *sln*, *fe*, *fr*, τ_c, *kr*, and *rsp.* Overall, the rainfall parameters (*rain*, *dur*, and *xip*) were the most sensitive variables from RHEM. The next important group of variables included the hydrologic parameters *ke* and *ns*.

Using figure 4, we can also investigate the effect of an input parameter over the entire parameter space. For example, the parameter *rain* had the highest mean value of sensitivity (5.13), which means that given a small increase in rainfall (5% in this study), the *soil loss* output will change by 5.13 times 5% on average. The maximum sensitivity index of *rain* was 23.48, which indicates that, in this extreme case, a small change in rainfall will induce a change in calculated *soil loss* of 23 times the percentage change in the rainfall amount. The minimum sensitivity of *rain* was 0.16, which indicates that a change in *rain* will induce a change in *soil loss* in all cases tested. The standard deviation of S_{rain} was 2.96, which was the largest value on the list. This indicated that the sensitivity to *rain* varied greatly from case to case, and the effect of *rain* on *soil loss* was highly interactive with other parameters.

Tiscareno-Lopez et al. (1994) conducted a sensitivity analysis on a similar soil erosion model (WEPP) on the

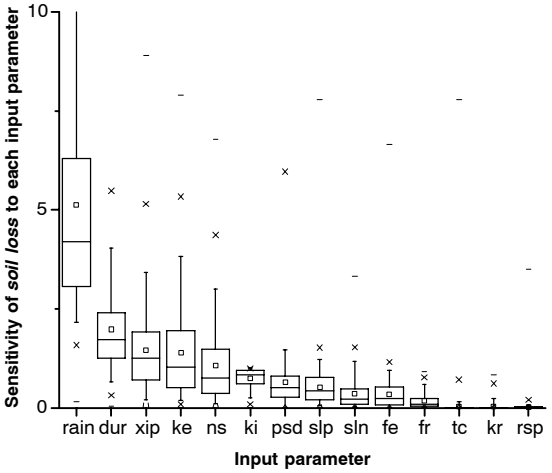

Figure 4. Statistics of absolute sensitivities for each input parameter. The sensitivity scale (*y*-axis) only shows values less than 10. The input parameters (*x*-axis) are ranked in order of mean sensitivity, which is represented by the small square symbols within the boxplots. Each S_i is represented as a boxplot. The box height indicates the 25th and 75th percentiles, the "x" symbols indicate the 5th and 95th percentiles, and the "–" symbols indicate the minimum and maximum values. The input parameters are described in table 1.

USDA-ARS Walnut Gulch Experimental Watershed located near Tombstone, Arizona. The results from his study indicated that, on that watershed, rainfall amount was the most sensitive parameter, followed by *ke*. From our results, *rain* was the most important parameter for 98.0% of events, followed by *slp*, *psd*, *ki*, τ_c, or *ke* depending on the combination of input values. From figures 3 and 4, we can see that RHEM is a complex model, whereby the localized sensitivities vary greatly from site to site.

Estimates of the sensitivity distributions can also be used to compare and classify the input parameters. A plot of the mean and standard deviation of each S_i is given in figure 5. This figure has often been used to classify the effects of parameters as a preliminary analysis (Morris, 1991; Saltelli and Campolongo, 2000; Francos et al., 2003). From figure 5, the input parameters can be generally classified into three groups: *rain* is alone in the first group with both the highest

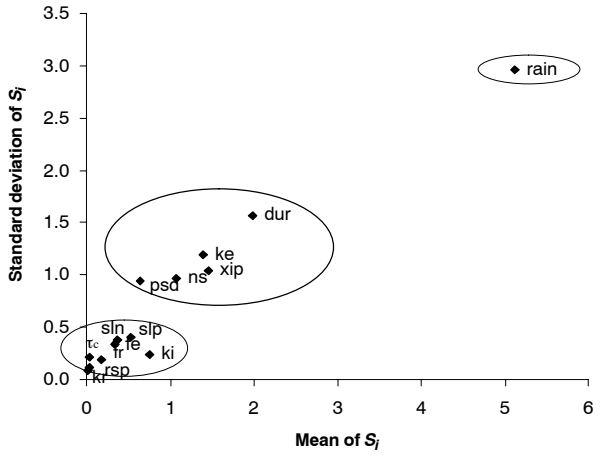

Figure 5. Plot of the estimated means and standard deviations of the distribution of S_i. This plot helps to classify the effect of each input parameter (Morris, 1991).

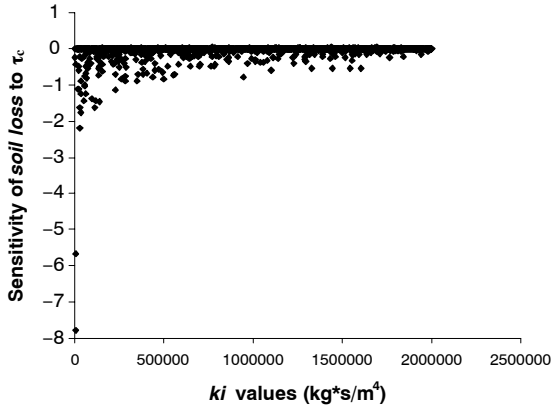

Figure 6. Plot of S_{τ_c} vs. *ki* values showing that τ_c may be very sensitive when *ki* is relatively small.

overall effect and the highest interaction or nonlinear effect; *dur*, *ke*, *xip*, *ns*, and *psd* are in the second group with median effects; and the rest of the parameters are in the third group, which contains the least important parameters.

Identification of Sensitive Regions

Identification of the sensitive regions could be very useful for both the model developer and model user. Ranking the sensitivity matrix by the sensitivity (S_i) to a parameter and then examining the continuity of the input parameter values is one way to locate the sensitive regions for this parameter. The distribution of these regions is dependent on the model complexity, the number of the input parameters, and the size of the parameter space. For a simple model with few input parameters, and especially when the sensitive regions tend to be tightly packed and well connected with a strong gradient within the parameter space (i.e., highly distinct from the non-sensitive regions), the sensitive regions may be easier to identify. For a complex model, such identification may be difficult, but the process may be made easier if the non-related parameters are removed from the matrix and or if the parameter space is redefined to a smaller subset of the full input parameter space. The framework of this method is simple and allows re-analysis of the sensitivities based on the smaller, newly defined parameter space of interest (fig. 1).

For example, the overall effect of critical shear stress (τ_c) is small, but based on the ranked sensitivity matrix by S_{τ_c}, we

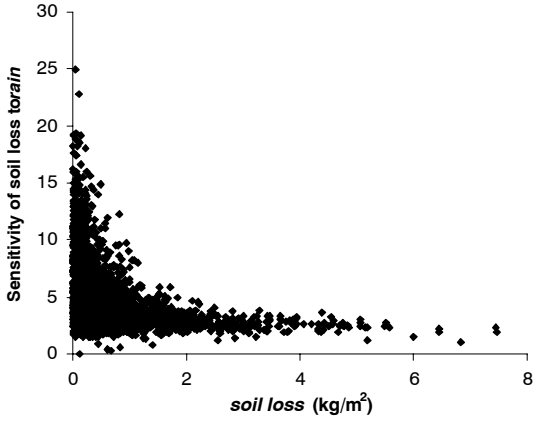

Figure 7. Sensitivity of *soil loss* to *rain* (S_{rain}) vs. magnitude of *soil loss*.

found that the model could be very sensitive to τ_c for some extreme events. Furthermore, in the ranked matrix, we found that the sensitivity to τ_c tended to be higher when *ki* was small. This is a reasonable relationship because a low *ki* means that interrill contributions to erosion will be insignificant, and that rill erosion will be far more important. Since τ_c affects rill erosion, it is reasonable that it is a very sensitive parameter for these situations. Figure 6 shows the relationship between S_{τ_c} and *ki*. The value of S_{τ_c} was not always high for all cases of small *ki* because S_{τ_c} also depended on the values of other parameters (particularly *kr* and τ_c itself).

Model Response Related to Output Values

A plot of the sensitivity index (S_i) versus the output values (*soil loss*) revealed the interesting fact that as the *soil loss* levels decrease, the sensitivities to the input parameters tend to increase. Figure 7 is an example of S_{rain} plotted against the *soil loss* values. The sensitivity indices for all the input values showed a similar relationship with *soil loss* values. This relationship indicates that there is more uncertainty involved for small *soil loss* events, which is consistent with the results of Nearing (2000), who showed that model predictions of erosion compared to field measurements show less relative error for larger magnitudes of measured erosion.

Relationship Between Sensitivities for Different Input Parameters

Figure 8 is a plot of S_{ki} versus S_{kr} that shows the relationship between the two parameters: the sensitivity for *ki* can be large only when the sensitivity for *kr* is low, and vice versa. This relationship makes sense because *soil loss* in RHEM is controlled by both interrill erosion and rill erosion, which are associated with *ki* and *kr*, respectively. The total *soil loss* is the summation of the *soil loss* from the rill area and the interrill area. If the interrill erosion accounts for the larger proportion of the total *soil loss*, then S_{ki} will be higher than S_{kr}. On the other hand, if the rill erosion accounts for the larger proportion, then the total *soil loss* will be more sensitive to *kr* than to *ki*. In addition to *kr*, rill erosion is also controlled by τ_c, and the contribution to erosion by rilling only occurs when the flow shear exceeds the critical hydraulic shear stress (τ_c).

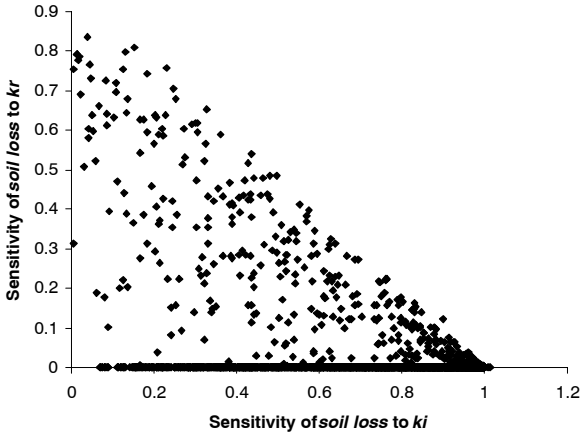

Figure 8. Plot of sensitivities of S_{ki} vs. S_{kr}.

In fact, 2,483 of the 3,180 events (78.08%) did not generate rill erosion, and S_{kr} and S_{τ_c} were both zero for these events. This explains why the overall sensitivity to *ki* (figs. 2 and 3) was greater than to *kr* and τ_c, and why figure 8 shows many points located at $S_{ki} = 1$. Furthermore, the sensitivity of *soil loss* to *ki* also depends on other parameters, such as *psd* and *fr* (see next section), and S_{ki} is not always 1 when S_{kr} and S_{τ_c} are 0.

Dependencies of Sensitivity Indices on Input Parameter Values

Regression analysis and correlation analysis were used to understand the dependence of the sensitivity for an input parameter on the parameter values (table 2). The coefficient of determination (R^2) of the regression describes the percentage of the variance of the sensitivity index that can be explained by the magnitudes of the input parameters. The correlation coefficients of S_i and the values of each input parameter reveal the dependence of S_i on each input parameter. For example, it can be seen from table 2 that approximately 50% of the variance of S_{fr}, S_{sln}, and S_{ke} can be explained by the magnitudes of the entire input parameter set. The correlation matrix in table 2 helps to further decompose this dependency. As can be seen, S_{fr} is dependent on parameters *kr* and *ki*; thus, the

Table 2. Dependencies of sensitivity indices on the input parameter values.

Input Parameters	Sensitivity Indices													
	S_{fr}	S_{sln}	S_{ke}	S_{ki}	S_{rain}	S_{ns}	S_{xip}	S_{fe}	S_{slp}	S_{dur}	S_{kr}	S_{psd}	S_{tc}	S_{rsp}
	R^2 of the regression of S_i on input parameter values													
	0.518	0.511	0.475	0.444	0.432	0.399	0.389	0.376	0.374	0.223	0.221	0.116	0.068	0.024
	Correlation coefficient of S_i to each input parameter													
slp	−0.172	0.247	0.084	−0.171	−0.134	0.057	0.050	0.148	0.009	0.060	0.079	0.352	−0.051	−0.005
sln	−0.217	−0.307	−0.190	−0.160	0.125	−0.110	−0.123	−0.187	0.278	0.060	0.015	−0.072	−0.012	0.035
rain	0.145	0.086	0.335	0.101	0.096	0.249	−0.072	0.036	−0.120	−0.036	−0.008	0.036	0.024	−0.026
dur	−0.127	0.043	−0.282	−0.061	−0.177	−0.135	0.154	0.014	0.033	−0.010	−0.015	0.003	−0.045	0.005
xip	0.162	−0.102	0.324	0.089	0.094	0.180	0.108	−0.063	−0.041	0.234	0.004	−0.006	0.029	0.004
ki	0.325	−0.109	−0.001	0.206	0.088	0.003	0.019	−0.045	−0.219	−0.093	−0.083	−0.409	0.096	−0.022
kr	−0.370	0.070	−0.018	−0.193	0.004	0.007	−0.001	−0.004	0.144	0.040	0.048	−0.004	−0.100	0.066
τ_c	0.166	−0.020	0.025	0.158	−0.014	−0.015	0.002	−0.030	−0.088	−0.034	−0.048	−0.002	−0.016	−0.027
ke	−0.060	−0.068	−0.438	−0.041	−0.099	−0.193	0.100	−0.023	0.041	0.011	−0.010	−0.027	−0.020	0.024
Ns	−0.051	−0.066	−0.241	−0.040	−0.103	−0.362	0.089	−0.014	0.035	0.032	−0.010	−0.031	−0.014	0.021
fr	−0.122	−0.346	−0.198	−0.095	0.134	−0.125	−0.133	−0.214	0.259	0.050	−0.003	−0.071	0.002	0.031
fe	0.265	−0.094	0.012	0.251	0.081	−0.003	0.015	−0.056	−0.185	−0.100	−0.087	−0.370	0.059	−0.015
rsp	−0.037	−0.039	−0.018	−0.098	0.003	0.021	0.001	0.038	0.019	0.029	0.030	−0.034	0.060	−0.044
psd	0.224	0.034	0.024	0.165	−0.020	0.006	0.012	0.024	−0.153	−0.025	0.013	−0.087	0.025	−0.010

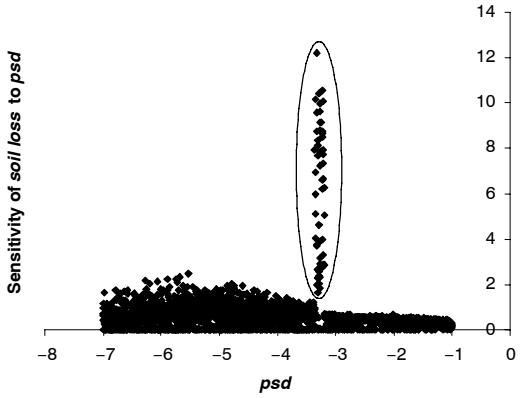

Figure 9. Scatter plot of sensitivity of soil loss to *psd* (S_{psd}) vs. *psd*, revealing a discontinuous model response when *psd* is close to −3.2.

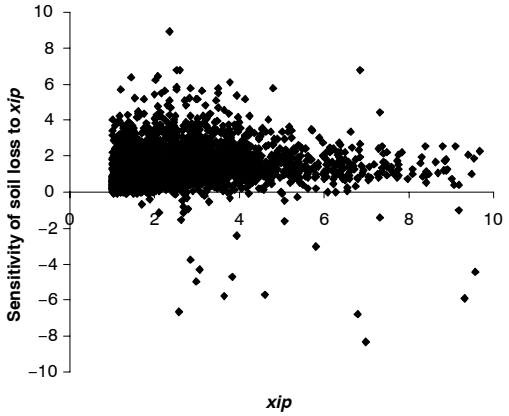

Figure 10. Scatter plot of sensitivity of soil loss to *xip* (S_{xip}) vs. *xip* values.

sensitivity of runoff friction (*fr*) is related to the magnitude of the erosion parameters.

The coefficients in table 2 reveal many insights into the relationships between the parameters. For example, S_{ns} and S_{ke} are dependent on the values of *rain*, *dur*, and *xip*. This relationship reflects the fact that runoff generation in RHEM is controlled by both the rainfall regime (associated with rainfall parameters *rain*, *dur*, and *xip*) and the infiltration regime (associated with hydrologic parameters *ke* and *ns*).

Table 2 also shows that there is negative correlation between S_{ke} and *ke*, which indicates that the response of *soil loss* to *ke* is dependent on the magnitude of *ke* itself. The negative correlation coefficient indicates that the higher the *ke* value, the greater the sensitivity for parameter *ke*. This relationship makes sense because a high *ke* value is often associated with a small amount of runoff and *soil loss*, and the sensitivity of *soil loss* to input parameters increases as the *soil loss* value decreases (as shown in fig. 7).

Scatter Plots to Identify Characteristics of Model Behavior

Scatter plots of the sensitivity index (S_i) at each point over the values of the *i*th parameter at this point can help the modeler survey the model response and identify nonlinear relationships, thresholds, and potential model problems. Figure 9 is a scatter plot of S_{psd} over the corresponding *psd* values. The parameter *psd* is important because it is the only parameter that accounts for particle size distribution in this study. Figure 9 is revealing because it shows an unexpected and undesirable model response around the *psd* value of −3.2. The same sensitivity procedures, focused on a narrow region of *psd* (−3.0, −3.4) for a closer look, confirmed the inconsistent model behavior. For example, for sediment with a *psd* of −3.31, a 5% increase in *psd* could induce a 70% increase in *soil loss*, which was much more sensitive than simulations with *psd* values outside this region. This is not a reasonable model response for this variable. A careful examination suggested that the cause of this problem is that the transport capacity was calculated based on different sediment particle sizes.

Another model problem was found by looking at the plot of S_{xip} over *xip* (fig. 10). According to the modeler's understanding of the erosion process and model structure, an increase in *xip* should only induce increases in *soil loss*; thus, S_{xip} should always be positive. However, figure 10 shows there are some situations where S_{xip} is negative, and they show up at various magnitudes of *xip*. A closer look at those points with negative S_{xip} values showed the general tendency that *xip* was more sensitive as the value of *xip* increased.

The cause of this problem was found by careful examination of one of the problematic events. In RHEM, the rainfall parameters (*rain*, *xip*, and *dur*) are read from an input file and transformed into a double-exponential hyetograph to simulate the time-step rainfall process. The parameter *rain* controls the total area under the hyetograph, *dur* controls the duration of the hyetograph, and *xip* controls the peak of the hyetograph. The hydrograph is calculated on a fixed time step based on the hyetograph and on the infiltration calculations. Water becomes available for runoff generation only when the rainfall rate at a time step exceeds the infiltration rate at the time step. Thus, the shape of the hyetograph and the infiltration curve control the duration and amount of runoff, and with the roughness, slope length, and gradient, they control the peak rate of runoff and consequent *soil loss* value.

The erosion model uses a double-exponential transformation approximation for creating the synthetic hyetograph from rainfall input values. Because of the way in which this done, there are a small number of combinations of the three rainfall parameters such that when the modeler increases *xip* and maintains constant values of *rain* and *dur*, the model in–

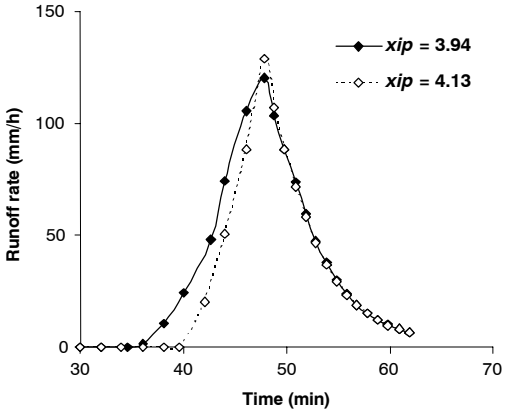

Figure 11. Hydrographs from rainfall events with the same *rain* (41.82 mm) and *dur* (47.83 min) but with different *xip* values. Due to the double-exponential transformation in the model, an increase in *xip* sometime causes an increase in rainfall peak and a decrease in rainfall at the beginning of the hyetograph. This distortion of the hyetograph may cause an observed decrease of runoff and *soil loss* corresponding with the increase in *xip*, explaining the unexpected negative S_{xip} values in figure 10.

creases the rainfall intensity peak but also reduces the rainfall amount at the beginning of the hyetograph. This small difference in the shape of the hyetograph can make a large difference in the hydrograph in a limited number of cases (fig. 10). Less runoff can be generated after the increase in *xip*, and the modeler can thus obtain a negative S_{xip} for these events. This also explains why the higher the *xip* value, the more sensitive *xip* becomes for points with negative S_{xip}, because the higher the *xip* value, the more distortion occurs at the beginning of the hyetograph. Figure 11 is an example of how increasing *xip* may induce a decrease in runoff. The total runoff amounts from the two events are 17.94 mm (*xip* = 3.94) and 14.81 mm (*xip* = 4.13), respectively.

The three examples above describe how scatter plots of local sensitivity indices over the local parameter values may help to identify nonlinear relationships, thresholds, and model problems. Scatter plots such as figures 9 and 10 are also very useful when the modeler is attempting to fix model problems, as shown in the flowchart (fig. 1).

Conclusion

A sensitivity analysis method based on the concept of local sensitivity and Latin hypercube sampling was conducted, using the soil erosion component in RHEM as a case study. The local sensitivity indices of *soil loss* to 14 input parameters of RHEM at 10,000 points from the full parameter space were obtained and used to build a sensitivity matrix. The sensitivity matrix was analyzed by correlation analysis and scatter plots to draw useful insights into model response and interactions between model parameters: (1) the results highlighted the importance of local sensitivity, which varies from site to site for a complex model such as RHEM; (2) these analyses showed the relative importance of different input parameters; (3) the results also showed the ability of the method to identify the sensitive range and relationships between input parameters; (4) the method was used to decompose the dependency of model response on input parameter values; (5) the method effectively detected model errors. The method described in this article can be used as an element of the iterative model development process whereby model response can be surveyed and problems identified and corrected in order to construct a robust model.

References

Alberts, E. E., M. A. Nearing, M. A. Weltz, L. M. Risse, F. B. Pierson, X. C. Zhang, J. M. Laflen, and J. R. Simanton. 1995. Chapter 7: Soil component. In *USDA Water Erosion Prediction Project: Hillslope Profile and Watershed Model Documentation.* D. C. Flanagan and M. A. Nearing, eds. NSERL Report No. 10. West Lafayette, Ind.: USDA-ARS National Soil Erosion Research Laboratory.

Breshears D. D., T. B. Kirchner, and F. W. Whicker. 1992. Contaminant transport through agroecosystems: Assessing relative importance of environmental, physiological, and management factors. *Ecological Applications* 2(3): 285-297.

Campolongo, F., and A. Saltelli. 1997. Sensitivity analysis of an environmental model: An application of different analysis methods. *Reliability Eng. System Safety* 57(1): 49-69.

Crosetto, M., and S. Tarantola. 2001. Uncertainty and sensitivity analysis: Tools for GIS-based model implantation. *Intl. J. Geographical Info. Sci.* 15(5): 415-437.

Elliot, W. J., A. M. Liebenow, J. M. Laflen, and K. D. Kohl. 1989. A compendium of soil erodibility data from WEPP cropland soil field erodibility experiments 1987 & 88. NSERL Report No. 3. West Lafayette, Ind.: USDA-ARS National Soil Erosion Research Laboratory.

Flanagan, D. C., and S. J. Livingston, eds. 1995. USDA Water Erosion Prediction Project: User summary. NSERL Report No. 11. West Lafayette, Ind.: USDA-ARS National Soil Erosion Research Laboratory.

Flanagan, D. C, and M. A. Nearing. 1995. *USDA Water Erosion Prediction Project: Hillslope Profile and Watershed Model Documentation*. NSERL Report No. 10. West Lafayette, Ind.: USDA-ARS National Soil Erosion Research Laboratory.

Francos, A., F. J. Elorza, F. Bouraoui, G. Bidoglio, and L. Galbiati. 2003. Sensitivity analysis of distributed environmental simulation models: Understanding the model behavior in hydrological studies at the catchment scale. *Reliability Eng. System Safety* 79(2): 205-218.

Helton, J. C. 1993. Uncertainty and sensitivity analysis techniques for use in performance assessment for radioactive waste disposal. *Reliability Eng. System Safety* 42(2-3): 327-367.

Hornberger, G. M., and R. C. Spear. 1981. An approach to the preliminary analysis of environmental systems. *J. Environ. Mgmt.* 12(1): 7-18.

Ionescu-Bujor, M., and D. G. Cacuci. 2004. A comparative review of sensitivity and uncertainty analysis of large-scale systems: I. Deterministic methods. *Nuclear Sci. Eng.* 147(3): 189-203.

Laflen, J. M., W. J. Elliot, R. Simanton, S. Holzhey, and K. D. Kohl. 1991. WEPP soil erodibility experiments for rangeland and cropland soils. *J. Soil Water Cons.* 46(1): 39-44.

Laflen, J. M., W. J. Elliot, D. C. Flanagan, C. R. Meyer, and M. A. Nearing. 1997. WEPP: Predicting water erosion using a process-based model. *J. Soil Water Cons.* 52(2): 96-102.

Liu, Y., H. V. Gupta, S. Soroochian, and L. A. Bastidas. 2004. Exploring parameter sensitivities of the land surface using a locally coupled land-atmosphere model. *J. Geophysical Res.* 109: D21101.

McKay, M. D., W. J. Conover, and R. J. Beckman. 1979. A comparison of three methods for selecting values of input variables in the analysis of output from a computer code. *Technometrics* 21(2): 239-245.

Morris, M. D. 1991. Factorial sampling plans for preliminary computational experiments. *Technometrics* 33(2): 161-174.

Nearing, M. A. 2000. Evaluating soil erosion models using measured plot data: Accounting for variability in the data. *Earth Surface Processes and Landforms* 25(9): 1035-1043.

Nearing, M. A., G. R. Foster, L. J. Lane, and S. C. Finkner. 1989. A process-based soil erosion model for USDA Water Erosion Prediction Project technology. *Trans. ASAE* 32(5): 1587-1593.

Saltelli, S. T., and F. Campolongo. 2000. Sensitivity analysis as an ingredient of modeling. *Stat. Sci.* 15(4): 377-395.

Simanton, J. R., M. A. Weltz, and H. D. Larson. 1991. Rangeland experiments to parameterize the Water Erosion Prediction Project model: Vegetation canopy cover effects. *J. Range Mgmt.* 44(3): 276-281.

Stein, M. 1987. Large sample properties of simulations using Latin hypercube sampling. *Technometrics* 29(2): 143-151.

Tiscareno-Lopez, M., V. L. Lopes, J. J. Stone, and L. J. Lane. 1994. Sensitivity analysis of the WEPP watershed model for rangeland: 1. Hillslope processes. *Trans. ASAE* 37(1): 151-158.